

Vol. 4 No. 2, Dec. 2024



FUAM

Journal of Pure and Applied Science

Available online at
www.fuamjpas.org.ng



An official Publication of
College of Science
Joseph Sarwuan Tarka University,
Makurdi.



Efficient Removal of Copper II and Lead II Ions from Single and Binary Solutions Utilizing Adsorbents from *Olea Europaea* Seed Shells

E.E. Mwenkoba

Department of Chemistry, Faculty of Physical Sciences, Joseph Sarwuan Tarka University Makurdi, Nigeria

*Correspondence E-mail: mwenkobaemmanuelzekiel@gmail.com

Received: 24/02/2024 Accepted: 25/04/2024 Published online: 29/04/2024

Abstract

Chemically activated and carbonized adsorbents prepared from *Olea europaea* seed shell (OES) were assessed for their capability to remove Cu (II) and Pb (II) ions from their single or binary aqueous solutions. The usage of adsorbents derived from *Olea Europaea* seed shells was found to be an efficient method for the removal of both Copper II and Lead II ions from single and binary solution systems. The adsorbents showed high adsorption capacity and selectivity towards these two heavy metal ions. The removal process was quick and highly effective, with a removal efficiency of over 90%. The adsorbents also showed excellent stability, making them a reliable choice for industrial and environmental applications. Additionally, the use of these adsorbents resulted in minimal waste production, making the process environmentally friendly. Overall, the results of this study suggest that utilizing adsorbents from *Olea Europaea* seed shells is a promising approach for the efficient and sustainable removal of Copper II and Lead II ions from contaminated solutions.

Keywords: Isotherms, adsorbents, characterization, thermodynamics, kinetics.

Introduction

In recent years, the contamination of water bodies by heavy metals, such as copper II (Cu^{2+}) and lead II (Pb^{2+}) ions has become a pressing environmental concern due to its detrimental effects on ecosystems and human health. Various industrial activities, mining operations, and urban runoff contribute significantly to the release of these toxic metals into the environment, necessitating effective remediation strategies to mitigate their impact [1-2].

Heavy metal contamination poses significant environmental and health hazards worldwide. Copper and lead, in particular, are known for their toxicity and persistence in the environment. Chronic exposure to these metals can result in severe health problems, including neurological disorders, developmental delays, and cardiovascular diseases. Furthermore, heavy metal pollution can disrupt ecosystems, degrade habitats, and threaten biodiversity [2].

Traditional methods for removing heavy metals from water, such as chemical precipitation and ion exchange, often have limitations in terms of efficiency, cost, and environmental sustainability. There is thus a growing interest in exploring alternative remediation techniques that are both effective and environmentally friendly [3]. Adsorption has emerged as a promising technique for the removal of heavy metals from aqueous solutions due to its simplicity, effectiveness, and versatility. Agricultural waste

materials, in particular, have garnered attention as potential adsorbents due to their abundance, low cost, and eco-friendliness. Among these materials, *Olea Europaea* (olive) seed shells represent a promising candidate for heavy metal adsorption owing to their inherent properties and availability as a byproduct of the olive processing industry [4-8]. The study is aimed at the aqueous phase adsorptive removal of lead and copper ions from their single and binary aqueous solutions using adsorbents prepared from OES biomass.

Materials and Method

Materials

All chemicals and reagents were of analytical grade and were used without further treatment. Copper nitrate pentahydrate, lead nitrate, were purchased from MACFES MERCHANDISE NIG.LTD, Jos, Plateau State.

Copper (II) nitrate pentahydrate [$\text{Cu}(\text{NO}_3)_2 \cdot 5\text{H}_2\text{O}$; $f_w = 277.63 \text{ g mol}^{-1}$] and lead(II) nitrate [$\text{Pb}(\text{NO}_3)_2$; $f_w = 331.20 \text{ g mol}^{-1}$] were separately oven-dried at 105°C for 24 h. One f_w of $\text{Cu}(\text{NO}_3)_2 \cdot 5\text{H}_2\text{O}$ is equivalent to 63.546 g of Cu; while a f_w of $\text{Pb}(\text{NO}_3)_2$ is equivalent to 207.200 g of Pb. Separate 2000-mg L^{-1} single-metal stocks of Cu and Pb were prepared by accurately weighed 8.7379g of dry $\text{Cu}(\text{NO}_3)_2 \cdot 5\text{H}_2\text{O}$ or 3.1969 g of the dry $\text{Pb}(\text{NO}_3)_2$ into a minimum volumes of deionized water in separate 250 cm^3 beakers and stirring gently for complete dissolution. The



contents of the beakers were transferred into separate 1 cm³ volumetric flasks with rinsing and the solutions made up to the mark. Working standards of the single-metal solutions: 50, 100, 150, 200 and 250 mgL⁻¹ were prepared by diluting 12.5, 25, 37.5, 50 and 62.5 mgL⁻¹ of the stocks to 500 cm³. Binary working standard solutions of 50, 100, 150, 200 and 250 mgL⁻¹ were prepared by conjointly diluting 12.5, 25, 37.5, 50 and 62.5 mgL⁻¹ of the single 2000 mgL⁻¹ Cu(II) and Pb (II) stocks to 500 cm³ in a volumetric flask. From the above weighed 8.7379g of dry copper (II) nitrate pentahydrate [Cu(NO₃)₂·5H₂O] and 3.1969g of dry lead nitrate [Pb(NO₃)₂] that were used to prepare their solutions, the mathematical proves that led to these figures are: the copper (II) nitrate pentahydrate [Cu(NO₃)₂·5H₂O] $f_w = 277.63 \text{ g/mol}$ and lead(II) nitrate [Pb(NO₃)₂]; $f_w = 331.20 \text{ g/mol}$. Their equivalent molar masses in their stock acid as stated above. Therefore, mass of copper (II) nitrate pentahydrate [Cu (NO₃)₂·5H₂O] will be $\frac{277.63 \text{ g/mol}}{63.542 \text{ g}} \times 2(\text{oxidation state}) = 8.7379 \text{ g}$ for Cu (II)

Mass of lead (II) nitrate [Pb(NO₃)₂] will be $\frac{331.20 \text{ g/mol}}{207.200 \text{ g}} \times 2(\text{oxidation state}) = 3.1969 \text{ g}$ for Pb(II)

Preparation of adsorbents from *Olea europaea* seed shells

Olea europaea seed shells (OES) were obtained from oil mills; from Fier District of Pankshin Local Government Area, Plateau State. The dried precursor was pulverized using mortar/pestle, and the resulting powder sieved using 2 mm sieve. The sieved material was activated according to the method adopted by [9], by steeping it in a saturated ammonium chloride solution for 24 h. The slurry was filtered and the residue rinsed repeatedly with distilled water and air-dried to serve as the chemically activated adsorbent (AOES). A portion of the AOES was pyrolyzed in a muffle furnace at 350 °C for 30 min. The resulting carbon was washed with deionized water to remove ash, air-dried and labelled as the carbonized adsorbent (COES).

Potential of hydrogen at zero point charge (pH_{zpc})

The potential of hydrogen at zero point charge (pH_{zpc}) is the pH of the suspension of the adsorbent at which the surface acidic (or basic) functional groups of an adsorbent no longer contribute to the pH value of the solution [10]. pH point of zero charge of the adsorbent was determined as reported by [11]. Separate aliquots 50 cm³ of 0.01 moldm⁻³ NaCl solution were measured into Erlenmeyer flasks. The pH of the solutions in the flasks was adjusted to values of 2, 4, 6 and 8 by adding 0.1 moldm⁻³ HCl or 0.1 moldm⁻³ NaOH solutions. Then 0.5g portions of AOES and COES, as the case may be, were added and agitated in a shaker for 1 h and then allowed to settle for 48 h to reach equilibrium at prevailing temperature; pH of the solutions were then determined. Plot of initial pH (pH₀) versus the difference between the initial and final pH

values (Δ pH) were plotted. The pH_{pzc} was taken as the point where Δ pH = 0.

Bulk density

Bulk density was determined using the tamping method of [12]. A 5g portion of the adsorbent was placed in a 10 cm³ measuring cylinder. The cylinder was tapped until it occupied a minimum volume. Apparent volume was read to the nearest graduated unit, the bulk density, ρ_b was calculated in (kgm⁻³) using equation (1):

$$\rho_b = m_a/V \quad (1)$$

Where m_a is the mass of adsorbent (kg) and V is the apparent volume (m⁻³).

Attrition

A 1.0g portion of the adsorbent was steeped in 50 cm³ of distilled water and the resulting slurry stirred for 2h, filtered and the residue air-dried at laboratory temperature. Attrition was calculated based on weight loss of the adsorbent after stirring; the mass of the residue was determined and then correlated to the original mass [13]. Loss on attrition was calculated as:

$$\text{Loss on attrition (\%)} = \left(\frac{m_i - m_f}{m_i} \right) \times 100 \quad (2)$$

where m_i is initial mass (g), m_f is final mass (g).

Preparation and standardization of 0.1 moldm⁻³ sodium thiosulphate solution

A 0.15g of pure dry potassium iodate was accurately weighed, and dissolved in 25 cm³ of cold, boiled-out distilled water, 2g of iodate-free potassium iodide and 5 cm³ of 1 moldm⁻³ sulphuric acid. The liberated iodine was titrated with the thiosulphate solution with constant shaking. When the colour of the liquid had turned pale yellow, it was diluted to 200 cm³ with distilled water. A 2 cm³ aliquot of starch solution was added, and the titration continued until the colour changed from blue to colourless. The titration was repeated with two other similar portions of potassium iodate [14].

Preparation and standardization 0.05 moldm⁻³ iodine solution

A 20g portion of iodate-free potassium iodide was dissolved in 30 - 40 cm³ of distilled water in a glass stoppered 1cm³ graduated flask. Exactly 12.7 g of resublimed iodine was weighed out on a watch glass on a rough balance (never on an analytical balance on account of the iodine vapour), and was transferred by means of a small dry funnel into the concentrated potassium iodide solution. Glass stopper was inserted into the flask, and shaken in the cold until all the iodine was dissolved. The solution was allowed to acquire room temperature, and was made up to the mark with distilled water. The iodine solution was preserved in amber coloured small glass-stoppered bottles, and was kept in a cool, dark place.



Next, 25 cm³ of the iodine solution was transferred to a 250 cm³ conical flask, diluted to 100 cm³ and the standard thiosulphate solution was added from burette until the solution turned pale yellow. A 2 cm³ of starch solution was added, and the addition of the thiosulphate solution continued slowly until the solution was just colourless, this procedure was repeated twice and average was taken [15].

Procedure for determination of iodine number/surface area

A 0.5g portion of the adsorbent was added to 25 cm³ of the standard iodine solution. The mixture was stirred vigorously for 10 min, and the slurry filtered. A 20 cm³ aliquot of the iodine filtrate was back-titrated against the standard thiosulphate. This procedure was repeated twice and average was taken [8]. The iodine number, n_{I_2} (i.e., amount in moles of iodine adsorbed per g adsorbent) was calculated using equation (3), while the adsorbent surface area, A (m²g⁻¹) was calculated using the modified equation (4) of [16]:

$$n_{I_2} (\text{mol.g}^{-1}) = \frac{C_t (V_b - V_s)}{2 \times 10^3 m_a} \quad (3)$$

$$A (\text{m}^2.\text{g}) = N_o \left\{ \frac{C_t (V_b - V_s)}{2 \times 10^3 m_a} \right\} \sigma_{I_2} \quad (4)$$

where C_t is the concentration of the thiosulphate (mol L⁻¹); V_b and V_s are respectively, the titre values of the blank and adsorbent-treated iodine solutions (L); m_a is mass of the adsorbent used (0.5 g); N_o is the Avogadro constant (6.02214 × 10²³ mol⁻¹); and σ_{I_2} is the cross-sectional area of an iodine molecule (3.2 × 10⁻¹⁹ m²).

Titrateable surface charge

A suspension of 1.0g of the adsorbent in 50 cm³ each of 0.1 moldm⁻³ NaOH, 0.1 moldm⁻³ Na₂CO₃ and 0.1 moldm⁻³ NaHCO₃ was stirred in a closed vessel for approximately 20 to 24 h. The slurry was filtered, 10 cm³ aliquot each was added to 15 cm³ standard 0.1 moldm⁻³ HCl solutions. The HCl neutralized the unreacted base. The solution was then back titrated with standard 0.1 moldm⁻³ NaOH, the volume of NaOH required to neutralize the sample was converted to titrateable negative surface charge [17]. Results were expressed in mm H⁺ ions neutralized by excess OH⁻ ions per g of adsorbent.

Fourier Transform Infrared (FT-IR) Spectroscopy

A small portion of the adsorbent was taken, and ground in a mortar until the sample had a glossy appearance, then about 2- 6 mg of KBr was added to the sample until a homogeneous blend was obtained. The scan was run using the FT-IR spectrometer with a model (Apodization Happ-Genzel) at NARICT IN Zaria, Kaduna State.

Quality Assurance/Control/Statistical Treatment of Analytical Data

In all cases, the residual Cu (II) and Pb (II) in solution were assayed by AAS. The actual amounts of the metal ions adsorbed were calculated using the mass balance relationship equation (5); while percentage removal was calculated by equation (6).

$$q_e = \frac{(C_o - C_e)V}{m} \quad (5)$$

$$\% \text{ Removal} = \frac{C_o - C_e}{C_o} \times 100 \quad (6)$$

Where C_o and C_e are the initial and residual metal ion concentrations (mgL⁻¹), respectively; V is the aliquot of Cu and Pb single or binary solution used (50 cm³); and m is the mass of adsorbent used for a particular batch treatment (0.5 g). The adsorption isotherms and adsorption kinetics parameters were derived from the appropriate algorithms using the MS Excel software.

Adsorption Studies

An adsorption isotherm essentially describes how the quantity of adsorbate adsorbed onto the surface of the adsorbent varies with the concentration of the adsorbate in the surrounding gas or liquid phase at a constant temperature [18]. There are several types of adsorption isotherms, each describing different behaviors in the adsorption process. Some common types include:

Langmuir isotherm

The Langmuir model is applicable in the cases where only one molecular layer of adsorbate is formed at the adsorbent surface which remains constant even at higher adsorbate concentrations [19]. The linearized Langmuir equation can be represented by equation (7):

$$\frac{C_e}{Q_e} = \frac{C_e}{Q_o} + \frac{1}{K_L Q_o} \quad (7)$$

where Q_e is the amount adsorbed (mg/g), C_e is the equilibrium concentration of the adsorbate (mg/L), Q_o (mg/g) is the maximum amount of adsorbate adsorbed per unit mass of sorbent corresponding to complete coverage of the adsorptive sites, K_L (L/mg) is the Langmuir constant related to the energy of adsorption. A linear plot

of $\frac{C_e}{Q_e}$ versus C_e gives the inverse of the slope as Q_o and

K_L from the intercept. The Langmuir model assumes that adsorption occurs at homogeneous sites and forms a monolayer. The characteristics of the Langmuir isotherm are determined by the dimensionless constant called separation factor, R_L expressed in equation (8):



$$R_L = \frac{1}{(1 + K_L C_0)} \quad (8)$$

where K_L (L/mg) and C_0 (mg/L) retain their usual meaning as stated earlier in equation 1. R_L indicates the nature of adsorption process such that $R_L > 1$, $R_L = 1$, $0 < R_L < 1$, and $R_L = 0$ indicate that adsorption is unfavourable, linear, favourable and irreversible, respectively.

Freundlich Isotherm

This model proposes heterogeneous energetic distribution of active sites, accompanied by interaction between adsorbed molecules. The linearized Freundlich is given by the equation (9), [20]:

$$\ln Q_e = \frac{1}{n_F} \ln C_e + \ln K_F \quad (9)$$

where Q_e (mg/g) is the amount of adsorbate adsorbed per unit mass of the adsorbent and C_e (mg/L) is the equilibrium concentration. K_F is a constant related to the adsorption capacity (Freundlich constant) and n_F is an empirical parameter related to the adsorption intensity which varies with the heterogeneity of the material [21]. A linear plot of $\ln Q_e$ versus $\ln C_e$ gives the slope of n_F and intercept K_F .

Thermodynamics Studies

Key thermodynamic parameters namely the Gibbs free energy change (ΔG), enthalpy change (ΔH) and entropy (ΔS) for the aqueous phase adsorptive removal of Cu(II) and Pb(II) ions were calculated using appropriate algorithms. The ΔG (J/mol) is given as:

$$\Delta G = -RT \ln K_L \quad (10)$$

Where R is the universal gas constant (8.314 J/mol.K), T is the temperature (K).

$$K_L \text{ (L/mol)} = K_L \text{ (L/mg)} \times 10^3 \text{ (mg/g)} \times A_r \text{ (g/mol)} \quad (11)$$

where A_r is the relative atomic weight of Cu and Pb (63.546 and 207.200 g/mol, respectively).

Since the unit for the RT term is J/mol, K_L in equation (5) must be dimensionless. Consequently, experimental values of K_L (L/mol) are made dimensionless by multiplying by 55.5 (moles of water per liter of solution). Accordingly, the correct expression for (ΔG°) is:

$$\Delta G^\circ = -RT \ln 55.5 K_L \quad (12)$$

Note that the term $55.5 K_L$ (L/mol \times mol/L) is dimensionless [22].

The enthalpy (ΔH) and entropy (ΔS) parameters are respectively estimated from the slope and intercept of the Van't Hoff equation (13):

$$\ln K_L = \frac{\Delta S^\circ}{R} - \frac{\Delta H^\circ}{RT} \quad (13)$$

where R and T retain their meaning as defined in equations. (4) and (6). Actual values of ΔH and ΔS are respectively obtained from the slope and intercept of the $\ln(55.5 K_L)$ versus ($10^3 \text{ K})/T$ plot.

Kinetics Studies

Most of the sorption/desorption processes of various solid phases are time dependent. To understand the dynamic interactions of pollutants with solid phases and to predict their fate with time, knowledge of the kinetics of these processes is important [23,24]; From kinetic analysis, the solute uptake rate determines the time required for completion of adsorption reaction. Various kinetic models have been used by various researchers [23,24].

Lagergren's pseudo-first-order model

Lagergren pseudo-first order is widely used to test the adsorption rate of an adsorbate from an aqueous solution. The Equation can be expressed as follows:

$$\ln(Q_e - Q_t) = \ln Q_e - k_1 t \quad (14)$$

Where Q_t is the amount of adsorbate adsorbed per unit of adsorbent (mg/g) at contact time t (min), Q_e (mg/g) is the amount of adsorbate adsorbed per unit mass of the adsorbent, k_1 is the pseudo-first order rate constant (L/min). A linear plot of $\ln(Q_e - Q_t)$ versus t gives the rate constant k_1 [25].

Blanchard pseudo-second-order model

[26] Presented the pseudo-second order kinetic in equation (15):

$$\frac{t}{Q_t} = \frac{1}{k_2 Q_e^2} + \frac{t}{Q_e} \quad (15)$$

Where k_2 is the pseudo-second order rate constant (g.mg⁻¹.min⁻¹). The initial adsorption rate, h (mg/g.min) and

$h = k_2 Q_e^2$. The slope from the linear plot of $\frac{t}{Q_t}$ versus t

gives the second order rate constant k_2 .

Weber-Morris intraparticle diffusion model

Weber-Morris intraparticle diffusion model could be expressed thus in equation (16):

$$Q_t = k_{id} \sqrt{t} + C \quad (16)$$

Where k_{id} is the intra-particle diffusion rate constant (mg g⁻¹ min^{-1/2}) and C is the intercept which describes the boundary layer thickness. The slope from the linear plot of



Q_t versus \sqrt{t} gives the intraparticle diffusion rate constant k_{id} [27].

Results and Discussion

Physicochemical Properties of Adsorbents

Table 1: Selected Physicochemical Properties of *Olea europaea* Seed Shell Adsorbents[†]

Attribute	AOES	COES
pH _{water} (solid:liquid = 1:100)	5.60 ± 0.02	6.10 ± 0.06
pH _{zpc}	2.65 ± 0.05	1.53 ± 0.08
Bulk density (kgm ⁻³)	629.33 ± 1.32	750.50 ± 1.41
Ash content (%)	8.70 ± 0.03	15.30 ± 0.10
Attrition (%)	7.00 ± 0.02	5.00 ± 0.04
Iodine number (×10 ⁻³ mol.g ⁻¹)	1.50 ± 0.03	1.93 ± 0.01
Iodine number (mg.g ⁻¹)	380.71 ± 1.22	489.85 ± 1.56
Surface area (m ² .g ⁻¹)	289.06 ± 1.05	371.92 ± 1.25
Total surface charge (mmol H ⁺ /g)	1.12 ± 0.01	1.33 ± 0.01

[†]**AOES** = chemically activated *Olea europaea* seed shells; **COES** = carbonized *Olea europaea* seed shells

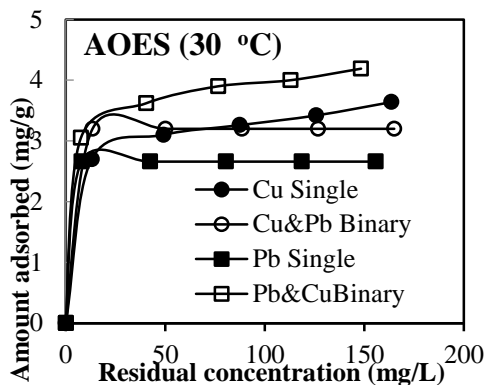


Table 2: Some Thermodynamic Parameters for the Removal of Cu(II) and Pb(II) Ions from Single and Binary Solutions Using Activated (AOES) and Carbonized (COES) *Olea europaea* Seed Shell Adsorbents at different Temperatures

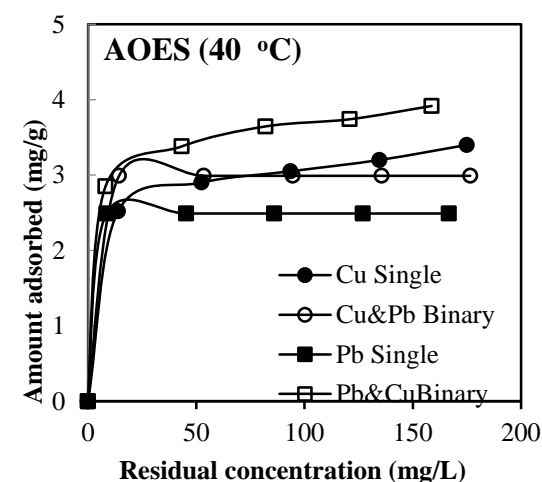
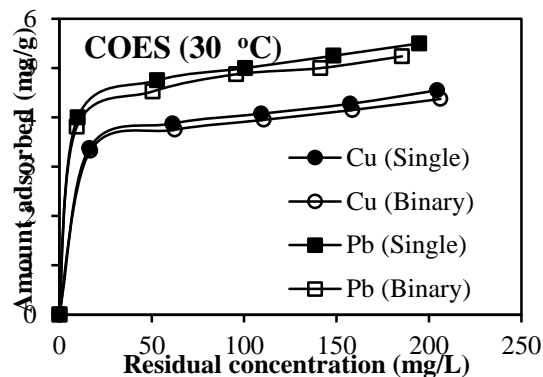
Adsorbent-Adsorbate System	T (K)	ΔG (kJ mol ⁻¹)	ΔH (kJ mol ⁻¹)	ΔS (JK ⁻¹ mol ⁻¹)
AOES-Cu-Single	303	-32.507	-20.860	39.009
	313	-33.439		
	323	-33.267		
AOES-Cu-Binary	303	-33.772	-36.898	-10.143
	313	-33.512		
	323	-33.737		
AOES-Pb-Single	303	-36.291	-22.805	45.527
	313	-37.712		
	323	-37.164		
AOES-Pb-Binary	303	-35.593	-4.132	107.001
	313	-37.603		
	323	-38.737		
COES-Cu-Single	303	-31.940	-2.785	96.110
	313	-32.849		
	323	-33.866		
COES-Cu-Binary	303	-32.127	-6.360	87.720
	313	-32.692		
	323	-33.834		
COES-Pb-Single	303	-35.817	-4.481	103.509
	313	-36.978		
	323	-37.937		
COES-Pb-Binary	303	-36.039	-6.194	96.438
	313	-37.017		
	323	-38.009		

Table 3: FT-IR Analysis

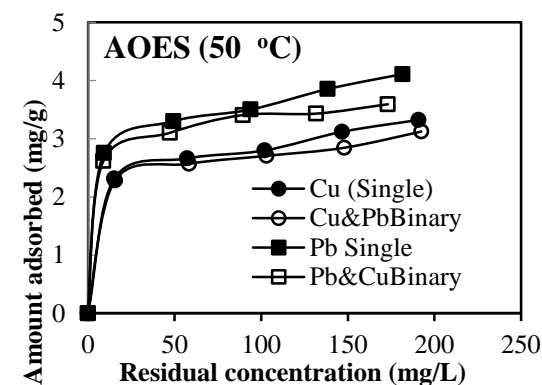
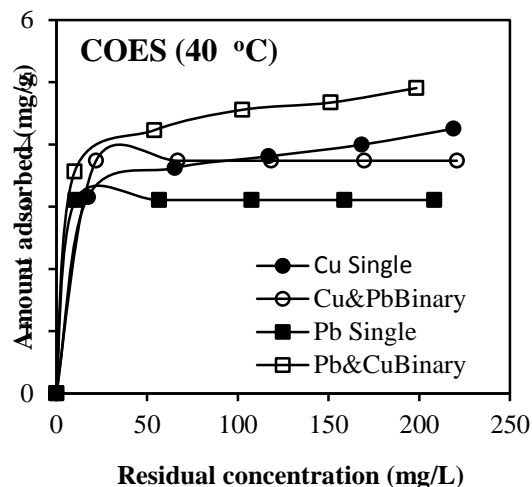
ν (cm ⁻¹)	Functional groups
3743	O-H, N-H
3512	O-H, N-H
3358	C-H
3265	C-H
1800	C=O
1750	C=O
1680	C=C
1440	S-O
1457	S-O
1050	C-O
775.41	C-H



(a)



(b)



(c)

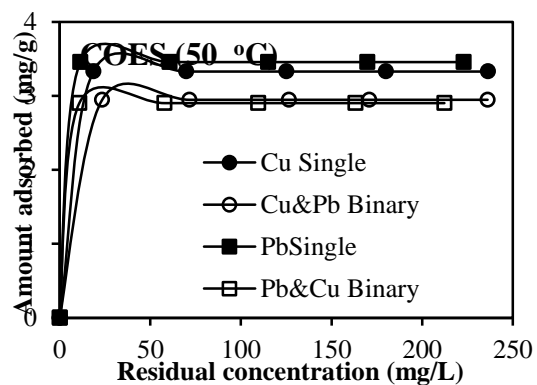


Figure 1: Isotherm Profiles for Removal of Cu (II) and Pb (II) Ions from Single and Binary Solutions using Activated (AOES) and Carbonized (COES) *Olea europaea* Seed Shell Adsorbents at Different Temperatures

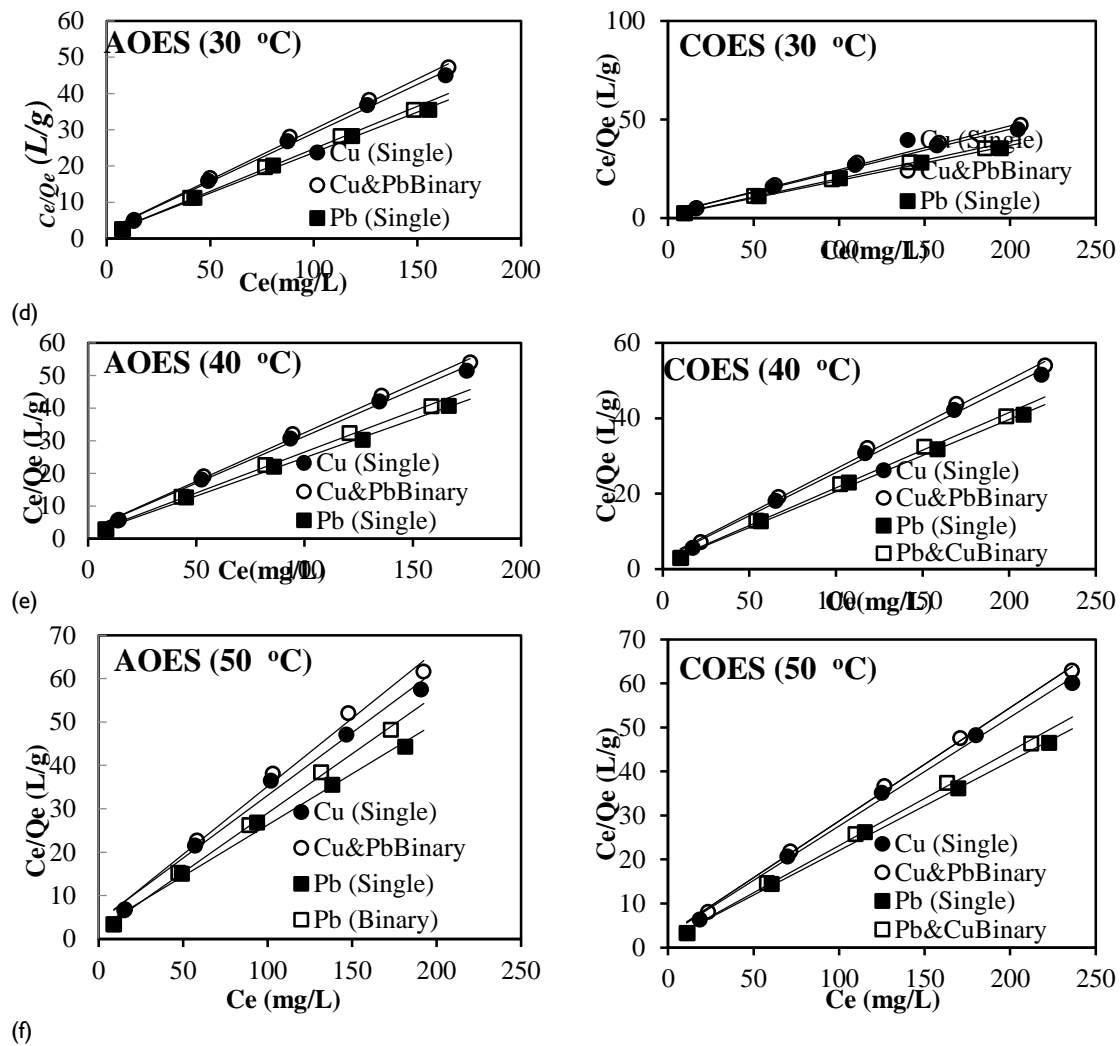


Figure 2: Linearized Langmuir Isotherms for Removal of Cu (II) and Pb(II) Ions from Single and Binary Solutions using Activated (AOES) and Carbonized (COES) *Olea europaea* Seed Shell Adsorbents at different Temperatures



Table 4: Langmuir Isotherm Parameters for Removal of Cu (II) and Pb (II) Ions from Single and Binary Solutions using Activated (AOES) and Carbonized (COES) *Olea europaea* Seed Shell Adsorbents at different Temperatures

Sorption system	Model Parameters	303 K	313 K	323 K
AOES-Cu (Single)	Q_o (mg.g ⁻¹)	3.745	3.497	3.472
	K_L (L.mg ⁻¹)	0.114	0.108	0.068
	$K_L (\times 10^3 \text{ L.mol}^{-1})$	7.244	6.863	4.321
	$55.5K_L$	402,042	380,897	239,816
	R^2	0.995	0.996	0.990
	R_L	0.149	0.156	0.746
AOES-Cu (Binary)	Q_o (mg.g ⁻¹)	3.597	3.367	3.195
	K_L (L.mg ⁻¹)	0.200	0.111	0.081
	$K_L (\times 10^3 \text{ L.mol}^{-1})$	12.709	7.054	5.147
	$55.5K_L$	705,350	391,497	285,659
	R^2	0.996	0.996	0.991
	R_L	0.091	0.153	0.198
AOES-Pb (Single)	Q_o (mg.g ⁻¹)	4.505	4.274	4.237
	K_L (L.mg ⁻¹)	0.157	0.171	0.089
	$K_L (\times 10^3 \text{ L.mol}^{-1})$	32.530	35.431	18.441
	$55.5K_L$	1,805,415	1,966,421	1,023,476
	R^2	0.997	0.998	0.992
	R_L	0.025 – 0.113	0.105	0.183
AOES-Pb (Binary)	Q_o (mg.g ⁻¹)	4.274	4.000	3.663
	K_L (L.mg ⁻¹)	0.177	0.164	0.160
	$K_L (\times 10^3 \text{ L.mol}^{-1})$	36.674	33.981	33.152
	$55K_L$	2,035,407	1,885,946	1,839,936
	R^2	0.998	0.998	0.998
	R_L	0.102	0.109	0.111
COES-Cu (Single)	Q_o (mg.g ⁻¹)	4.673	4.367	4.049
	K_L (L.mg ⁻¹)	0.091	0.086	0.085
	$K_L (\times 10^3 \text{ L.mol}^{-1})$	5.783	5.465	5.401
	$55K_L$	320,957	303,308	299,756
	R^2	0.995	0.995	0.996
	R_L	0.180	0.189	0.190
COES-Cu (Binary)	Q_o (mg.g ⁻¹)	4.505	4.237	3.891
	K_L (L.mg ⁻¹)	0.095	0.081	0.085
	$K_L (\times 10^3 \text{ L.mol}^{-1})$	6.228	5.147	5.401
	$55.5K_L$	345,654	285,659	299,756
	R^2	0.996	0.996	0.998
	R_L	0.174	0.198	0.190
COES-Pb (Single)	Q_o (mg.g ⁻¹)	5.618	5.236	4.951
	K_L (L.mg ⁻¹)	0.130	0.129	0.116
	$K_L (\times 10^3 \text{ L.mol}^{-1})$	26.936	26.729	24.035
	$55.5K_L$	1,494,948	1,483,293	1,333,943
	R^2	0.997	0.998	0.998
	R_L	0.133	0.134	0.147
COES-Pb (Binary)	Q_o (mg.g ⁻¹)	5.348	5.000	4.673
	K_L (L.mg ⁻¹)	0.142	0.131	0.122
	$K_L (\times 10^3 \text{ L.mol}^{-1})$	29.422	27.143	25.278
	$55.5K_L$	1,632,921	1,506,437	1,402,929
	R^2	0.998	0.997	0.997
	R_L	0.123	0.132	0.141



Discussion

Physicochemical Properties of *Olea europaea* Seed Shell Adsorbents

Both AOES and COES samples showed attributes that were generally comparable. AOES and COES had pH_{water} of 5.60 and 6.10, respectively. Corresponding values for pH_{zpc} were 2.65 and 1.53, respectively. Adsorbents with pH_{water} 6 – 8 are acceptable for applicability for water and wastewater treatment [28] and so, COES fits in here as far as the pH requirement is concerned. Bulk densities of 629.33 and 750.50 kg/m^3 , respectively were recorded for AOES and COES. These values are higher than those reported for ammonium chloride-activated and carbonized *Moringa oleifera* seed shells [29]. Bulk density gives an estimate of packing volume of an adsorbent implying that, an adsorbent with high bulk density gives an idea of volume activity and suggests better quality performance. Percent attrition (abrasion number), an indicator of the mechanical strength of an adsorbent for liquid phase applications was higher for AOES (7.00%) than COES (5.00%) with both values lower than their *Moringa oleifera* seed shells analogues. These values are interpretive of optimum mechanical strength implying its low degradability during handling and ease of regeneration and reactivation [30].

Iodine numbers (mg/g) and surface areas (m^2/g) respectively were 380.71 and 489.85 for AOES; 289.06 and 371.92 for COES. Adsorbents with high iodine number/surface area perform better in the removal of small sized contaminants. The surface charge of 1.12 $\text{mmol H}^+\text{eq/g}$ for AOES and 1.33 $\text{mmol H}^+\text{eq/g}$ for COES indicate favourable adsorption behaviour. The total surface charge gives an indication of the acidic and basic functional groups on the adsorbent's surface. Different oxygen-based acidic functional groups are present on the surface of activated carbons which include carboxyl groups, phenolic hydroxyls, quinine-type carbonyls, lactones, carboxylic acid anhydrides, ethers and cyclic peroxides [31,32].

FT-IR analysis assists to identify individual surface functional groups which may play key role in adsorption mechanism and capacity. Typically peaks attributable to O–H, N–H, C–H, C=O, C=C, S – O, C–O were recorded. Overall, the FTIR frequency shifts indicate that Cu (II) and Pb(II) were bound to the adsorbents via hydroxyl, amine, carboxylic, hydrogen bonding and aldehydic groups.

Adsorption Studies

Effect of initial metal ion solution concentration on removal of Cu (II) and Pb(II) – Isotherm profiles and models

Equilibrium data from sorption experiments are usually presented in the form of an isotherm, which mathematically or graphically displays the ratio of sorbed to non-sorbed solute per mass of adsorbent at constant

temperature. In this study, Figure 1 presents isotherms for the aqueous phase removal of Cu (II) and Pb (II) from their single and binary solutions using AOES and COES. All isotherms were operated at metal ion initial concentrations [$50 \leq C_0$ (mg/L) ≤ 550], solid/liquid ratio = x, $\text{pH} = x$, and contact time = x.

The isotherm profiles are noteworthy because for a particular adsorbent-adsorbate system, they reveal information about the adsorption process. Based on the classification by [8], the isotherms for both Cu (II) and Pb (II) adsorption onto AOES and COES in both single and binary solutions were typically L-shaped, indicating that the forces of interaction between Cu (II)-Cu (II), Pb(II)-Pb(II) or Cu(II)-Pb(II) ions are negligible relative to those between the metal ions and adsorbents. Overall, this observation implies that the activation energy of adsorption of the metal ions would be independent of surface coverage. Furthermore, the shape of the isotherm may also indicate the type of porosity present. The slightly sloping plateau of the isotherms suggests that AOES and COES are associated with a wide range of microporosity with some contribution from mesoporosity [33].

For the AOES adsorbent, at the temperature range (303 – 323 K) investigated in this study, ranges of Langmuir parameters: Q_0 (mg/g), K_L ($\times 10^3 \text{ L/mol}$), and R_L for single solution scenarios were: AOES-Cu ($3.472 \leq Q_0 \leq 3.745$), ($4.321 \leq K_L \leq 7.244$) and ($0.034 \leq R_L \leq 0.746$), respectively. Corresponding ranges for the AOES-Pb sorption systems were: ($4.237 \leq Q_0 \leq 4.505$), ($18.441 \leq K_L \leq 32.530$) and ($0.023 \leq R_L \leq 0.183$). For the binary solution systems, ranges of the Langmuir parameters were: AOES-Cu ($3.195 \leq Q_0 \leq 3.597$), ($5.147 \leq K_L \leq 12.709$) and ($0.020 \leq R_L \leq 0.198$), respectively. Corresponding ranges for the AOES-Pb sorption systems were: ($3.663 \leq Q_0 \leq 4.274$), ($33.152 \leq K_L \leq 36.674$) and ($0.022 \leq R_L \leq 0.111$).

For the COES adsorbent, ranges of Langmuir parameters: Q_0 (mg/g), K_L ($\times 10^3 \text{ L/mol}$), and R_L for single solution scenarios were: COES-Cu ($4.049 \leq Q_0 \leq 4.673$), ($5.401 \leq K_L \leq 5.783$) and ($0.042 \leq R_L \leq 0.190$), respectively. Corresponding ranges for the COES-Pb sorption systems were: ($4.951 \leq Q_0 \leq 5.618$), ($24.043 \leq K_L \leq 26.936$) and ($0.030 \leq R_L \leq 0.147$). For the binary solution systems, ranges of the Langmuir parameters were: COES-Cu ($3.891 \leq Q_0 \leq 4.505$), ($5.147 \leq K_L \leq 6.228$) and ($0.040 \leq R_L \leq 0.198$), respectively. Corresponding ranges for the COES-Pb sorption systems were: ($4.673 \leq Q_0 \leq 5.348$), ($25.278 \leq K_L \leq 29.422$) and ($0.027 \leq R_L \leq 0.141$).

Overall, Q_0 , K_L and R_L decreased with increase in temperature, indicating that the adsorptive removal of Cu (II) and Pb(II) was less favorable at higher temperatures. Actual values of the Langmuir parameters were correspondingly higher for metal ion-COES than the metal ion-AOES sorption systems, qualifying COES as the more potent of the experimental adsorbents. The values of R_L



are within the range ($0 \leq R_L \leq 1$) of favorable metal ion adsorption for both adsorbents [34].

Thermodynamics Analysis

Some thermodynamic parameters for the removal of Cu (II) and Pb(II) ions from their single and binary solutions using AOES and COES adsorbents at different temperatures are recorded in Table 2.

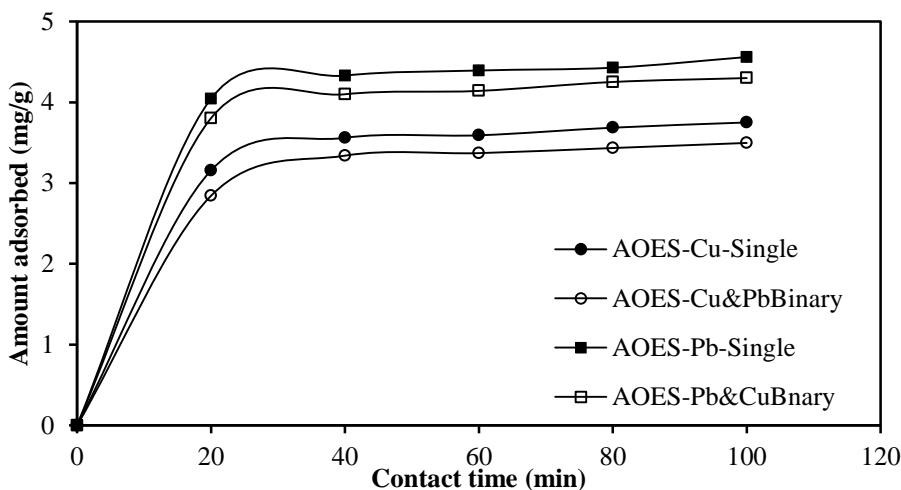
For the single solute systems ranges of ΔG (kJ/mol), ΔH (kJ/mol) and ΔS (J/K.mol) were: AOES-Cu (-33.077, -20.800, and 39.009); AOES-Pb (-37.056, -22.808 and 45.527); COES-Cu (-32.885, -2.785 and 96.110) and COES-Pb (-36.911, -4.481 and 103.509). Corresponding thermodynamic parameters for binary solution scenarios were: AOES-Cu (-33.673, -36.898, and 45.881); AOES-Pb (-37.244, -4.132 and 107.001); COES-Cu (-32.884, -6.360 and 87.720) and COES-Pb (-37.022, -6.194 and 96.438). The typically negative values of ΔH for all the sorption systems are interpretive of the exothermicity of the adsorption process. The enthalpy parameter can be used to differentiate between physisorption and chemisorption. From the literature, ΔH values [$-83 \leq \Delta H$ (kJ/mol) ≤ -830] represent chemisorption; while those in the range [$-8 \leq \Delta H$ (kJ/mol) ≤ -25] signify physisorption [26]. The ΔH values recorded in this study indicate that the adsorption of Cu (II) and Pb(II) onto AOES and COES is physisorptive in nature. The positive values of entropy change, ΔS (kJ/mol), indicates an increase in the degree of disorder, hence the spontaneous nature of Cu (II) and Pb (II) adsorption on AOES and COES. The negative values of ΔG

(kJ/mol) for adsorption of Cu (II) and Pb (II) on both experimental adsorbents represents the spontaneity of the adsorption process. From literature, ΔG values [$-20.00 \leq \Delta G^\circ$ (kJ/mol) ≤ 0.00] represent physisorption; while those in the range [$-400.00 \leq \Delta G$ (kJ/mol) ≤ -80.00] indicate chemisorption [35]. The ΔG values recorded in this study values are supportive of the physisorption mechanism

kinetics Analysis

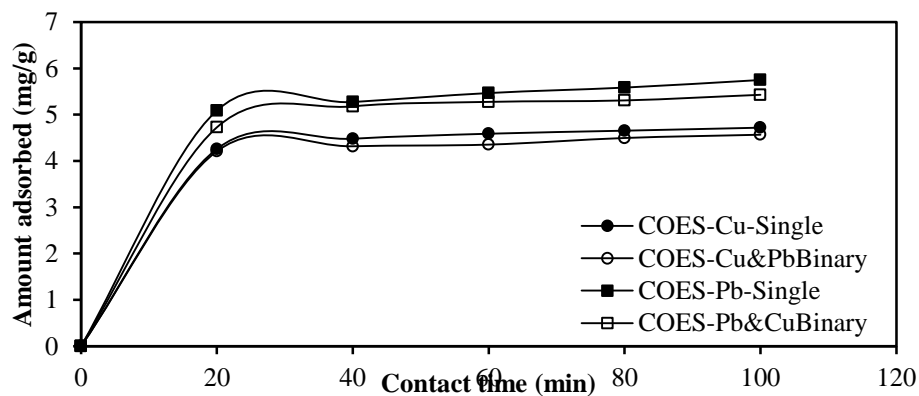
An important adsorption parameter derivable from equilibrium considerations is called the adsorption capacity. Another parameter of equal importance, the adsorption time (defined as the time taken to remove one-half of the initial concentration of the adsorbate), is used for defining an adsorbent and selecting appropriate operating conditions for the design of a wastewater treatment scheme [36]. Rate curves for aqueous phase removal of Cu (II) and Pb(II) by AOES and COES are illustrated in Figure 6.

For both AOES and COES, metal ion removal increased very rapidly within the first 20 min but decelerated beyond this point, gradually rendering slightly sloping plateaux at higher contact times, implying that the process would not offer additional kinetic advantage when contact times longer than 2 h were employed. Removal rates were generally higher for corresponding COES than AOES treatments. They were also higher for the single solution than the binary solution scenarios, furnishing higher removal of Pb (II) than Cu(II) for all scenarios.



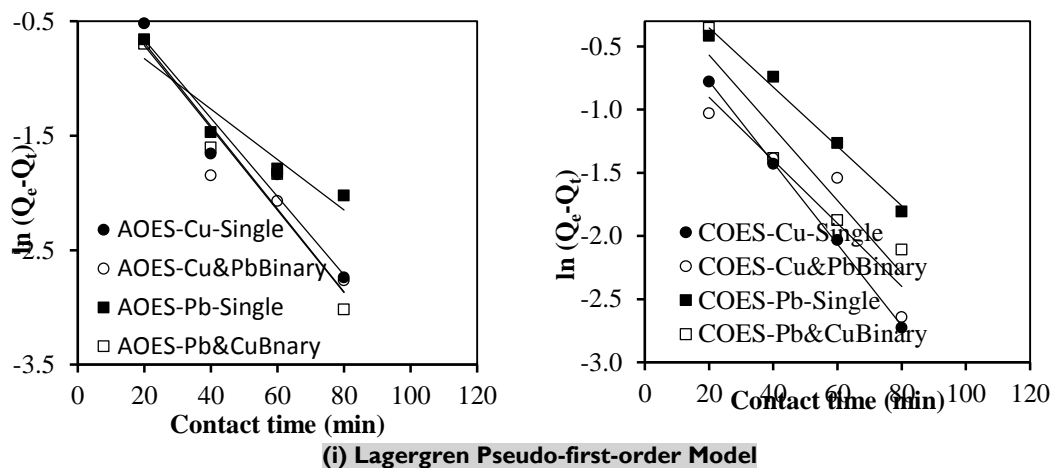


(g)

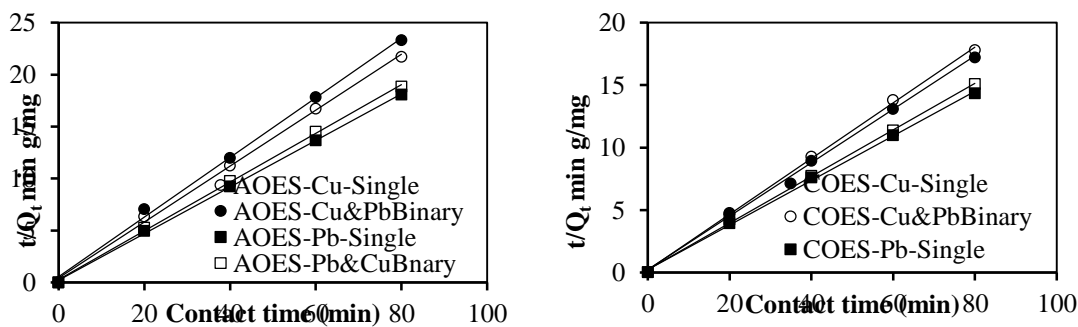


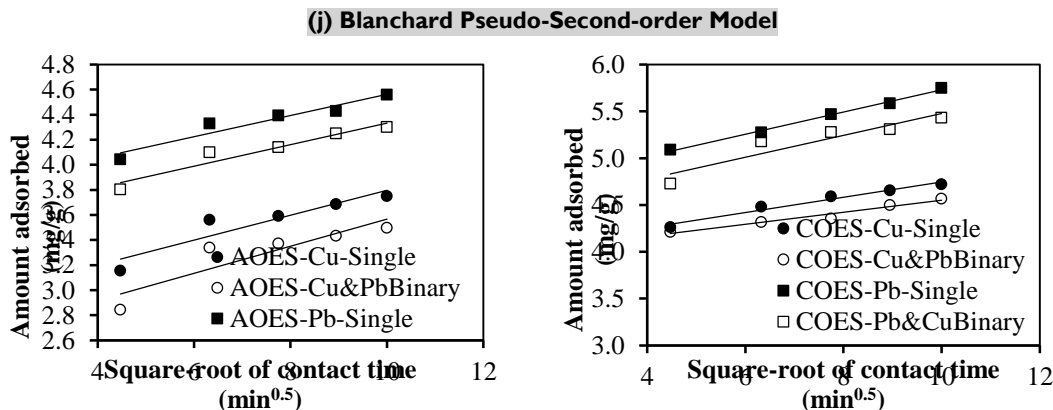
(h)

Figure 6: Rate Curves for Removal of Cu(II) and Pb(II) Ions from Single and Binary Solutions Using Activated (AOES) and Carbonized (COES) *Olea europaea* Seed Shell Adsorbents



(i) Lagergren Pseudo-first-order Model





(k) Weber-Morris Intraparticle Diffusion Model
Figure 7: Kinetic Model Plots for the Removal of Removal of Cu(II) and Pb(II) Ions from Single and Binary Solutions Using Activated (AOES) and Carbonized (COES) *Olea europaea* Seed Shell Adsorbents

Table 5: Kinetic Model Plots for Removal of Cu(II) and Pb(II) Ions from Single and Binary Solutions Using Activated (AOES) and Carbonized (COES) *Olea europaea* Seed Shell Adsorbents

Adsorbent- Adsorbate System	Model Parameters		Blanchard		Weber-Morris	
	Lagergren k_1 (min^{-1})	R^2	k_2 ($\text{g.mg}^{-1}\text{min}^{-1}$)	R^2	k_{id} ($\text{mg.g}^{-1}\text{min}^{-1/2}$)	R^2
AOES-Cu-Single	-0.034	0.938	0.163	0.998	0.099	0.873
AOES-Cu-Binary	-0.036	0.905	0.149	0.997	0.107	0.807
AOES-Pb-Single	-0.022	0.914	0.237	0.999	0.084	0.922
AOES-Pb-Binary	-0.036	0.944	0.188	0.998	0.085	0.927
COES-Cu-Single	-0.032	0.999	0.202	0.999	0.081	0.970
COES-Cu-Binary	-0.025	0.805	0.256	0.999	0.064	0.957
COES-Pb-Single	-0.023	0.987	0.141	0.998	0.118	0.994
COES-Pb-Binary	-0.028	0.910	0.156	0.999	0.116	0.875

Conclusion

Chemically activated and carbonized adsorbents prepared from *Olea europaea* seed shell (OES) were assessed for their capability to remove Cu (II) and Pb(II) ions from their single or binary aqueous solutions. The comminuted precursor was steeped in a saturated ammonium chloride solution for 24 h to furnish the chemically activated adsorbent (AOES). An aliquot of AOES was pyrolyzed in a muffle furnace at 350°C for 30 min to yield the carbonized adsorbent (COES). Both AOES and COES adsorbents showed favorable physicochemical attributes (pH, bulk density, attrition, iodine adsorption number/surface area, titratable surface charge and FTIR analysis). The influence of operational variables: concentration (50 – 250 mg/L), temperature (30 – 50°C) and contact time (0 – 120 min) on metal ion removal rate/efficiency were evaluated via batch adsorption experiments. The equilibrium adsorption data revealed L-shape isotherm profiles, implying that interactions between metal ions were of less importance than adsorbent-metal ion interactions. Linearized Langmuir isotherms revealed that across the temperature range considered, maximum adsorption capacities (mg/g) were recorded for single metal ion solutions for COES (Cu = 4.049 – 4.673; Pb = 4.951 – 5.618). Values of Gibbs free energy change, enthalpy change and entropy change revealed that the adsorption of Cu (II) and Pb(II) was

feasible, spontaneous, exothermic and followed the physisorption mechanism. Adsorption rate curves showed that metal ion removal increased very rapidly within the first 20 min but decelerated beyond order and pseudo-second-order kinetics and followed the intraparticle diffusion mechanism. The results may find applications in simple water and wastewater treatment schemes that utilize the principle of adsorption mechanism.

References

- [1] Baig, K. S., Doan, H. D., & Wu, J. (2009). **Multicomponent isotherms for biosorption of Ni^{2+} and Zn^{2+}** . *Desalination*, 249(1), 429-439.
- [2] Carvajal-Flórez, E., & Cardona-Gallo, S. A. (2019). **Technologies applicable to the removal of heavy metals from landfill leachate**. *Environmental Science and Pollution Research*, 26, 15725-15753.
- [3] Tan, I. A. W. Ahmed, A. L. and Hameed, B. H. (2018), **Adsorption of basic dye using activated carbon prepared from oil palm shell: batch and fixed bed studies**. *Desalination*, 225, 1328.



- [4] Mohan, D and Pittman C. U. Jr (2000). **Asenic removal from water/water waste using adsorbents- A critical review.** *Journal of Hazard Mater.*, 142, ppl-53
- [5] Xu, M., & McKay, G. (2017). **Removal of heavy metals, lead, cadmium, and zinc, using adsorption processes by cost-effective adsorbents.** *Adsorption processes for water treatment and purification*, 109-138..
- [6] Hung, Y. T., Wang, L. K., & Shamas, N. K. (Eds.). (2012). **Handbook of environment and waste management: air and water pollution control** (Vol. 1). *World Scientific*.
- [7] Fierro, V., Muniz, G., Gonzalez-Sanchez, G., Ballinas, M. L., and Celza, A. (2012). **Asenic removal by iron-doped activated carbons prepared by ferric chloride forced hydrolysis.** *Journal of Hazard Mater.*, 168 pp430-437
- [8] Kurniawan, T. A. and Babel, S. (2013). **Adsorption of Lead (II) from Aqueous Solutions onto Activated Carbon Prepared from Algerian Dates Stones of Phoenix Dactylifera. L (Ghars Variety) by H₃PO₄ Activation.** *Oriental Journal of Chemistry*. 30,1317-132 <https://doi.org/10.13005/ojc/300349>
- [9] Okieimen, F. E., Okieimen, C.O. and Wuana, R.A. (2007). **Preparation and characterization of activated carbon from rice husks.** *Journal of Chemical Society, Nigeria*. 32(1):126-136
- [10] Onwu, F.K. and Ogah, S.P.I. (2010). **Studies on the effect of pH on the sorption of cadmium (II), nickel (II), lead (II) and chromium (VI) from aqueous solutions by African white star apple (Chrysophyllum albidum) shell.** *African Journal of Biotechnology*, 9(42):7086-7093.
- [11] Abia, A.A. and Asuquo, E.D. (2008). **Sorption of Pb (II) and Cd (II) ions onto chemically modified and unmodified oil palm fruit fibre adsorbent: Analysis of pseudo second order kinetic models,** *Indian Journal of Chemical Technology*, 15: 341-348.
- [12] Ahmedna, M., Marshall, W.E., and Rao, R.M. (2000). **Granular activated carbons from agricultural by-products: preparations, properties and applications in cane sugar refining.** *Bulletin of Louisiana State University, Agricultural Centre*. 54.
- [13] Toles, C.A., Marshall, W.E., Johns, M.M., Wartelle, L.A. and McAloon, A. (2000). **Acid- activated carbons from almond shells: physical, chemical and adsorptive properties and estimated cost of production.** *Bioresource Technology*, 71:87-92
- [14] Vogel, A.I. (2000). **A textbook of quantitative inorganic analysis**, 6th edition, ELBS, London. Pp 431-440.
- [15] RAHMAN, M. H. A. (2020). **Rice husk activated carbon with NaOH activation: physical and chemical properties.** *Sains Malaysiana*, 49(9), 2261-2267.
- [16] Baccar, R., Bouzid, J., Feki, M and Montiel, A., (2009), **Preparation of activated carbon from Tunisian olive-waste cakes and its application for adsorption of heavy metal ions.** *Journal of Hazardous Materials*, 162, 1522-1529.
- [17] Van Winkle, S.C. (2000). **The effect of activated carbon on the organic and elemental composition of plant tissue culture medium,** Ph.D Dissertation, *Institute of paper Science and Technology, Atlanta Georgia*. P 64.
- [18] Shoemaker, D.P., Garland, C.W. and Nibbler, J.W. (1989). **Experiments in physical chemistry,** McGraw-Hill publishing company, NY; p. 353.
- [19] Langmuir, I. (1918). **The Adsorption of Gases on Plane Surfaces of Glass, Mica, and Platinum.** *Journal of American Chemical Society*. 40: 1361-1403
- [20] Mohammadi, A. S., Sardar, M., & Almasian, M. (2016). **Equilibrium and kinetic studies on the adsorption of penicillin G by chestnut shell.** *Environmental Engineering & Management Journal (EEMJ)*, 15(1).
- [21] Milonjić, S. K. (2007). **A consideration of the correct calculation of thermodynamic parameters of adsorption.** *Journal of the Serbian chemical society*, 72(12), 1363-1367.
- [22] Bansal, R.C. and Goyal, M. (2005). **Activated carbon adsorption.** Boca Raton, Crc Press Taylor and Francis Group. 6000 Broken Sound Parkway NW, Suite 300 Boca Raton, FL, U.S.A pp. 33487-2742. fixed bed column. *Journal of Hazardous Materials*, 161, 1427- 1435.
- [23] Sparks, D.L. (1989). **Kinetics of soil chemical processes.** Academic press, San Diego, CA. Sparks.
- [24] Sparks, D. L., & Suarez, D. L. (1991). **Rates of soil chemical processes.** SSSA special publication (USA), (27).
- [25] Lagergren, S. (1898). **About the theory of so-called adsorption of soluble substances.**
- [26] Ho, Y. S. and McKay, G. , (1999), **Pseudo-second order model for sorption processes,** *Process Biochem*, 34, 451-465.83
- [27] Badmus, O., Audu, K and Anyata, U. (2007). **Removal of lead ion from industrial wastewater by activated carbon prepared from periwinkle shells (Typanotonus fuscatus),** *Turkish Journal Engineering Environmental Science*. 31: 251-263.
- [28] Rajendran, A. B., Manivannan, G., Iothivenkatachalam, K., & Karthikeyan, S. (2015). **Characterization studies of activated carbon from low cost agricultural waste: Leucaena leucocephala seed shell.** *Rasayan J Chem*, 8(3), 330-338.
- [29] Wuana, R.A., Okieimen, F.E., Adejo, S.O. and Mbasugh, P.A. (2009). **Single and competitive aqueous**



- phase adsorption of calcium and magnesium ions onto rice husk carbon**, *Journal of Chemical Society of Nigeria*, 34(1):97 – 109.
- [30] Mahmoud, D.K., Salleh, M.A.M. and Abdul Karim, W.A.W. (2012). **Characterization and evaluation agricultural solid wastes as adsorbents: A review**, *Journal of Purity, Utility and Reaction of the Environment*, 1: 451–459.
- [31] Duru, C. E., Duru, I. A., Ogbonna, C. E., Enedoh, M. C., & Emele, P. (2019). **Adsorption of copper ions from aqueous solution onto natural and pretreated maize husk: adsorption efficiency and kinetic studies**, *Journal of Chemical Society of Nigeria*, 44(5).
- [32] Van Winkle, S. C. (2000). **The effect of activated carbon on the organic and elemental composition of plant tissue culture medium** (Doctoral dissertation, Georgia Institute of Technology).
- [33] Maheshwari, M., Vyas, R.K. and Sharma, M. (2013). **Kinetics, equilibrium and thermodynamics of ciprofloxacin hydrochloride removal by adsorption on coal fly ash and activated alumina**, *Desalination and Water Treatment*, 51(37-39): 7241-7254
- [34] Dula, T., Siraj, K, and Kitte, S.A. (2014). **Adsorption of hexavalent chromium from aqueous solution using chemically activated carbon prepared from locally available waste of bamboo (*Oxytenanthera abyssinica*)**, *ISRN Environmental Chemistry*, 2014, 1-10.
- [35] Marshall, W.E., Wastelle, D.H., Boler, D. E., Johns, M.M. and Toles, C.A. (1999), **Enhanced metal adsorption by soyabean hulls modified with citric acid**, *Bioresour. Technol.*, 69(3), 263-268.
- [36] Giles, C.H., Smith, D. and Huitson, A. (1974). **A general treatment and classification of the solute adsorption isotherm I. Theory**, *Journal of Colloid and Interface Science*, 47(3):755-765.

Cite this article

Mwenkoba E.E. (2024). Efficient Removal of Copper II and Lead II Ions from Single and Binary Solutions Utilizing Adsorbents from *Olea Europaea* Seed Shells. *FUAM Journal of Pure and Applied Science*, 4(2):6-20

© 2024 by the author. Licensee **College of Science, Joseph SarwuanTarka**



University, Makurdi. This article is an open access article distributed under the terms and conditions of the [Creative Commons Attribution \(CC\) license](https://creativecommons.org/licenses/by/4.0/).